Self-Assembly of a Swarm of Autonomous Boats into Floating Structures

Ian O'Hara, James Paulos, Jay Davey, Nick Eckenstein, Neel Doshi, Tarik Tosun, Jonathan Greco,
Jungwon Seo, Matt Turpin, Vijay Kumar and Mark Yim

Abstract— This paper addresses the self-assembly of a large team of autonomous boats into floating platforms. We describe the design of individual boats, the systems concept, the algorithms, the software architecture and experimental results with prototypes that are 1:12 scale realizations of modified ISO shipping containers, with the goal of demonstrating self-assembly into large maritime structures such as air strips, bridges, harbors or sea bases. Each container is a robotic module capable of holonomic motion that can dock in a brick pattern to form arbitrary shapes. Over 60 modules were built of varying capability. The docking mechanism is designed to be robust to large disturbances that can be expected in the high seas. The docking mechanism also incorporates adjustable stiffness so that the conglomerate can comply to waves representative of sea state three, and have the ability to dynamically stiffen as required. The component modules for autonomous assembly, docking and simultaneous collision-free planning as well as the software architecture are presented along with the description of experimental verification.

I. INTRODUCTION

Large robotic self-assembled aquatic structures enable capabilities such as the formation of offshore bases for humanitarian aide to hurricane stricken islands, ad hoc landing strips, encircling oil spills, or refueling depots in the middle of the ocean [1]. A large number of modified standard ISO shipping containers, which conform to a standard, low cost form factor easily transported around the world, can be used to form a swarm of autonomous boats that could be used to join together to form *Modular Sea Bases* (MSB) which can in turn be delivered nearly anywhere on the planet that container ships can reach.

This work describes the design of individual boats, the systems concept, the algorithms, the control and planning software and the software architecture of working with up to 60 modules at 1:12 scale. We will use the term *module* or *boat* to refer to the modified containers. With such large numbers, there are questions of how the modules self-organize, plan and execute motions that avoid collisions, while achieving the goal conglomerate shape (e.g. a harbor that conforms to the shoreline or a floating landing strip).

Self-assembly of autonomous agents (mobile agents docking with each other) has been a research problem in the self-reconfigurable robot research community for nearly two

decades, and there are a variety of approaches [2], [3]. However, the unique geometric and environmental constraints of this system require a new planner.

Modular sea bases were examined in [4] as a potential way to build Mobile Offshore Bases focusing on a large seaport or air base afloat at sea and movable under its own power. These systems could create bases where none exist which could be particularly useful for rapidly developing events. The modules were relatively large; in one version, the modules were 280 m long and they proposed assembling five of them end to end to form a landing strip. As in this paper, a scale model was constructed and examined, though at 1:150 scale and tethered [5]. They tested three modules that formed a chain, but did not have to deal with assembly of larger numbers of modules into complex shapes.

II. SYSTEM ARCHITECTURE

At the highest level, the system is split into three components: a fleet of boats, a central computer, and a poolside camera array (see Fig. 1). The fleet of boats consists of independent actors which are unaware of the others and are responsible for fulfilling requests from the central computer. The central computer consists of a number of loosely coupled software components which, working together, are responsible for taking an assembly blueprint and giving orders to the boats to assemble the specified conglomerate. Finally, the camera array provides boat pose feedback for all boats to the central computer and the boats themselves.

This paper first describes the implemented hardware design. It then goes on to describe a software system capable of both controlling the boats and assembling the conglomerates autonomously from a blueprint. Next, to address concerns about the destructive effects of a varying sea environment, analysis is done on conglomerate dynamics and on the docking mechanism of the boats. Finally, experiments in a pool are described that verify system capabilities.

III. HARDWARE

1) Propulsion: Each shipping container in the full-sized system is capable of holonomic motion. Our scaled system modules produce holonomic motion using four thrusters positioned in the corners of each scaled shipping container. Each thruster uses a 'water wheel' style design consisting of a spinning paddle and a water guide that produces a jet of water in one of two fixed directions (see Fig. 2). Boats capable of holonomic motion eases trajectory following and performing docking maneuvers. Making fine maneuvers with the boats also enables more precise station keeping against currents, waves or wind effects.
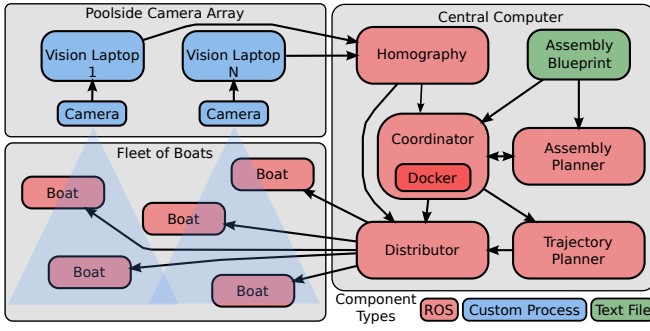
Fig. 1: System components are physically distributed across a central computer, vision laptops, and independent boats

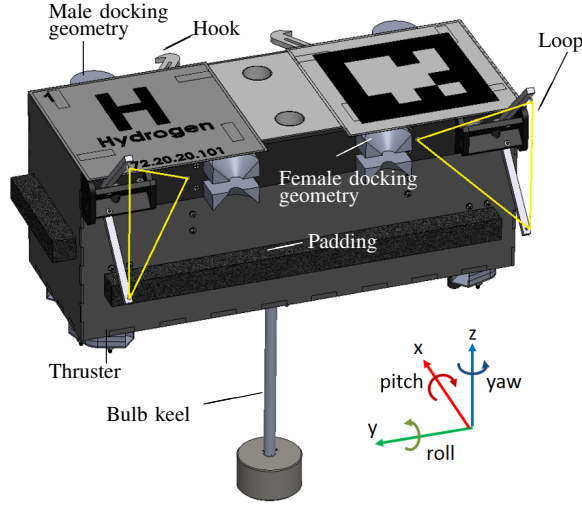Fig. 2: Tactically Expandable Maritime Platform module

(a) Female   (b) Male

Fig. 3: Docking mechanisms. (a) Loop detail fully extended, (b) Hook detail showing sweep.

2) Docking: The implemented docking concept was conceived by General Dynamics and QinetiqNA who constructed the full-sized ISO container prototype. It is a male to female connection mechanism for connecting modules together under dynamic wave conditions. One long side of the module is a male side and the opposing long side is a female side. The male side includes a hook sweeping in the horizontal plane that catches a suspended vertical cable on the female side of another module. Spring loaded folding arms (female side) are used to hold out a loop of string for the hook to catch. A motor winches both ends of the string at once on a spiraled winch drum (Fig. 3a) to allow the spring loaded arms to move out at the same time and at a non-linear speed during the docking process (outlined in Sec.IV-D). Additionally, if modules in the scaled system are located in the docked position, but the docking mechanisms are not engaged, the modules can still dock. A constant force spring located in the hook allows the hook mechanism to comply in the situations where the sweeping hook interferes with a close neighboring module.

Note that this docking mechanism results in a brick wall pattern as can be seen in Figs. 11, 12. Although the mechanism does not allow short-end to short-end attachments, general 2D shapes can be constructed [6]. An algorithm that plans for the assembly sequence for a given goal shape is described in Sec. IV-B.
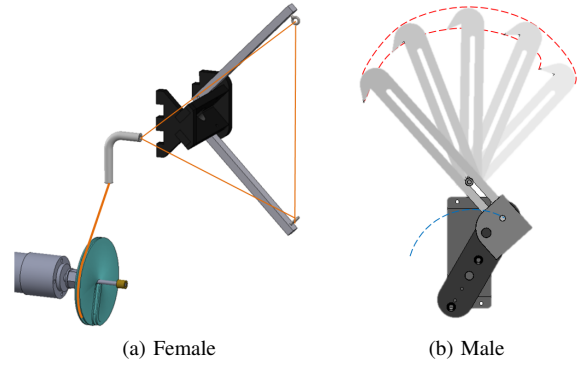
When docked, the interface between two modules includes padding on the sides of the hull. This padding lets structures made from the floating modules flex which is important to survive rough sea conditions as explained in Sec.V-B. The winches in the female side of the docking mechanism can pull two modules tighter, squeezing the padding to provide a controlled stiffness between modules.

3) Stability: Our scaled system modules were built with many components sitting well above the hull bottom resulting in a high center of mass. The boats also have low density resulting in a large freeboard. This combination makes the modules prone to large pitch and roll motions with the possibility of overturning. In addition, large roll and pitch introduce errors in the localization when using overhead cameras. For these reasons the scaled modules were given a bulb keel to keep the modules upright and resistant to roll. This bottom feature is likely not needed on the full sized boats, which will have a much lower freeboard height.

4) Electrical Design: All of the electronics on an individual boat are controlled by a Linux compatible Gumstix computer-on-module [7], which is mounted on a custom breakout board. The Gumstix was chosen for its size and to take advantage the Linux infrastructure (networking, development tool chain, drivers, etc). Using Linux also allowed easy integration with ROS [8]. The Gumstix controls two motors with built-in encoders to actuate the winches (Fig. 3a), two analog servos to move the hooks (Fig. 3b), and four motors used for propulsion of the boat. All six motors are controlled using off-the-shelf high current drivers, and are connected to the main processor with TTL serial. A bidirectional voltage translation board is necessary for the Gumstix (at 1.8 V logic) to send and receive control signals to all actuators (at 3.3 V and 5 V logic). A central PCB connects the Gumstix, all of the actuators, a leak sensor, and an externally visible LED board together and routes power to them from NiMH batteries.

IV. SOFTWARE

The overall control architecture required for autonomous operation spans multiple software components and multiple physical platforms. At the highest level, the Coordinator is responsible for sequencing operation of the Assembly Planner, the Trajectory Planner, and the Docking Routine.
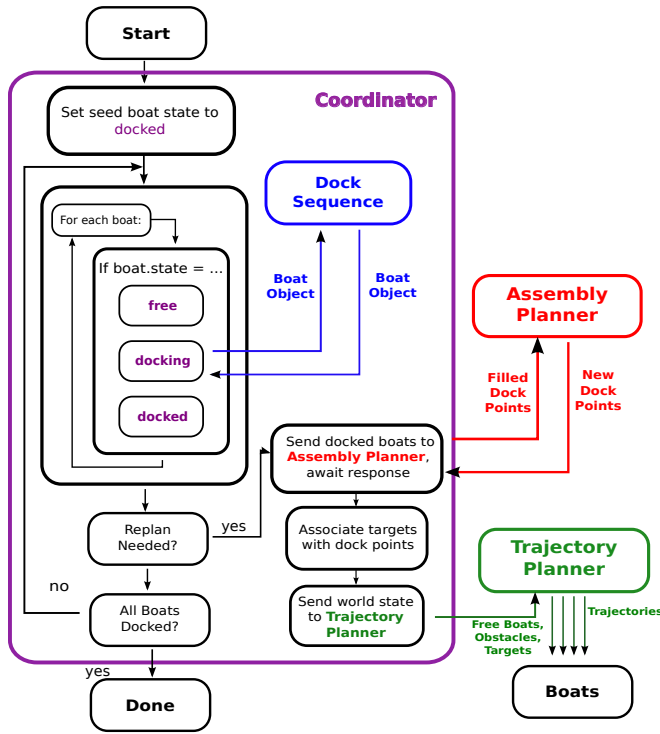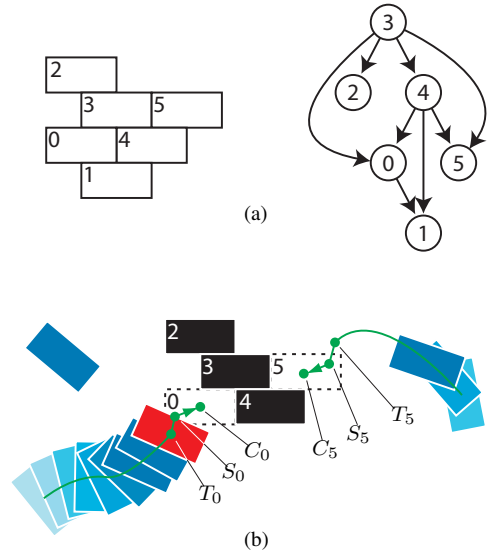
Fig. 4: Coordinator Operation

Fig. 5: (a) A shape with six sites (left), and its assembly sequence (right). (b) One state in the assembly where `boat.state` (Fig. 4) is `free`, `docking`, and `docked` for the blue, red, and black boats, resp. The red boat has reached T_0, target point of site 0, and has just changed to `docking`.

These components reside physically within a central computer, as sketched previously in Fig. 1. Each boat is a semi-independent agent which responds to infrequent trajectory commands and rapid pose estimates. A full scale field deployment might utilize radio for communication and GPS for localization. In our experiments a local wifi network provides communication managed by a Distributor Node, and overhead cameras publish pose estimates.

A. Coordinator

The Coordinator, outlined in Fig. 4, is an event-based state machine that allows the Assembly Planner, Trajectory Planner, and Docker to operate with some degree of asynchrony. The Coordinator parses a blueprint for the desired configuration and stores an internal map of *dock sites*, boat locations within the desired conglomerate (see the left panel of Fig. 5a). As construction progresses, the Assembly Planner identifies open dock sites that may be simultaneously filled and that will not later block the assembly sequence. Near each available dock site the Coordinator assigns a *target point*, a global coordinate where the centroid of a boat should be driven in preparation for docking (see Fig. 5b). The Coordinator passes the current locations of free boats, target points, and static obstacles to the Trajectory Planner, which then computes paths for free boats to reach the target points. Whenever a boat reaches a target point, the Coordinator passes control to the reactive Docking Sequence which maneuvers the boat into the corresponding dock site by actuating the hooks and winches to complete the dock. Whenever a dock site is successfully occupied, the Coordinator notifies the Assembly Planner so that it may expose more dock sites for continued assembly.

B. Assembly Planner

The Assembly Planner parses a blueprint for the desired configuration and generates an assembly sequence that specifies an order for filling the dock sites. The sequence can be executed interactively as mentioned in Sec. IV-A: the Assembly Planner takes as input, the shape of the current structure and returns open dock sites that can be occupied around the current structure. The algorithm [6] is briefly summarized here. First, a goal shape is represented as a single connected collection of dock sites to be occupied by boats (the left panel of Fig. 5a). After arbitrarily designating one of the dock sites as a *seed*, dock site 3 in this example, we construct a directed graph on the collection of the dock sites such that its edges represent local-scale assembly precedences (the right panel of Fig. 5a). The resultant graph is guaranteed to be acyclic; we then obtain an assembly sequence that can be executed without infeasible, cyclic dependency. As a result, the structure grows as a single connected component from the boat occupying the seed with multiple boats docking in a parallel distributed manner. For example, at the instant shown in Fig. 5b where dock sites 3, 2, and 4 are occupied, free boats can occupy dock sites 0 and 5 without mutual communication. Filling the dock sites is independent according to the assembly sequence shown in the right panel of Fig. 5a. Moreover, following the resultant sequence guarantees reachability: there exists a feasible path into any open dock site that is not blocked by the structure. For example, consider a structure composed of dock sites 0, 1, and 3 in the example; to occupy dock site 4, a boat has to pass through the narrow corridor between the boats occupying dock sites 3 and 1. The algorithm avoids such difficult to maneuver configurations. The time complexity of the algorithm is $O(m^2)$ where m is the number of the dock sites of a given goal shape.

C. Trajectory Planner

The Trajectory Planner is responsible for planning paths for free boats to reach the target point for open dock sites. In this way it provides the logical interface between the high level discrete reasoning of the Coordinator and the low level feedback controller embedded on the boats. A plan request from the Coordinator specifies the current locations of free boats, target points, and static obstacles as inputs to the planner. The Trajectory Planner then assigns free boats to specific target points and generates collision-free trajectories for the boats to reach their respective target points (Fig. 5b). Globally optimal plans are generated through our deterministic algorithm presented in [9]. Solution paths lay on a visibility graph constructed over the static obstacles, providing a fixed margin against collision. The time-dependent motion along these paths further ensures no collisions between moving boats by construction. Planning for ten boats is completed in less than one second, and those plans are then published as messages to the Distributor Node, which in turn sends individual trajectories to each boat. Replanning is required only when a boat successfully occupies a dock site, which results in the change of the current structure and the discovery of new docking sites by the Assembly Planner. The discrete nature of event-triggered plan requests and the capability of the boats to execute their assigned trajectories unattended significantly reduces the communication between the Coordinator and the many boats.

D. Docking Routine

When the Coordinator observes that a boat has reached its target point, control of the boat is passed to the Docking Routine. The Docking Routine resides within the Coordinator node and executes a tuned sequence of actions to bring the boats from the `dock_ready` state to the `successfully_docked` state. There are four stages to the docking sequence. *(1)* Starting from the target point (labeled T_0 and T_5 in Fig. 5b), approach the *standoff point*, an intermediate position for proper docking alignment (labeled S_0 and S_5). *(2)* Station-keep to stabilize position and open the winches or hooks on both boats. *(3)* Approach the dock site centroid (labeled C_0 and C_5) and close the winch or hook on both boats. *(4)* Evaluate dock success.

The routine is dynamic, with the docking boat driving forward to move its hook or winch into the capture region of the stationary boat. Appropriate hook and winch positions and the resulting capture region were experimentally determined through dry testing (Fig. 7). Additional parameters affecting docking success included stabilization time (in step *(2)*), the approach vector (step *(3)*), and error tolerance and wait times when evaluating success (step *(4)*). These parameters were tuned through docking tests in water.

Some dock attempts are rendered unsuccessful by disturbances (waves in the pool), or by localization or control errors. For example, if docking boats are too close when the hook fires, it will miss the loop. In this case, the hook will push against the hull of the other boat and cause them to drift apart without connecting. Failures are automatically detected by comparing the relative positions of the docking boats to the expected positions for success. In the case of failure, a spiral search is implemented where one boat relocates to a

different starting position and executes the sequence again. This changes the boat's approach vector and provides an additional chance for a successful dock.

E. Localization System

Sensing boat poses is done using APRIL Tags [10] via the cv2cg package [11]. Fiducial markers are placed on each boat, and are sensed by one or more cameras located above the pool surface. These cameras are mounted to a frame 3.7 m above the pool and 1.0 m out. The viewing frustum sees boats in a 12.8 m by 3.7 m rectangle that spans the entire width of the pool resulting in approximately 2 cm precision.

Each camera is attached via USB to a dedicated laptop running cv2cg and gives pose information for each boat's tags at 20-30 Hz. These laptops transmit the tag poses in their respective camera frames via UDP to the central computer. The central computer then uses prerecorded calibration information to project these coordinates into the single pool frame coordinate system, generating the (x,y,θ) coordinates for each boat. These world coordinates are then published over the ROS framework for the system components to use.

F. System Administration and Networking

Developing the Coordinator, Trajectory Planner, Assembly Planner, and code on dozens of floating boats is challenging. To do this, each boat automatically connects to known system wifi networks. Code development occurs on local machines, using a series of bash scripts that utilize rsync, ssh pipes, and tmux [12] sessions running on the boats to compile, run, and debug code simultaneously on all of the boats, the central computer, and the vision laptops. For boats that contain up to date binaries, turning on their power switch is enough for them to start their ROS node and become fully functional within the system.

Most of the system utilizes ROS for both p2p networking setup and data serialization/deserialization (see Fig.1). ROS was chosen over alternatives [13], [14] because it provides both serialization and p2p networking in one cohesive package, along with an extensive suite of self introspection tools (eg: rostopic, rosnode [15]). Also, the node and topic abstractions provide a convenient mechanism for debugging system components by replacing other components with "virtual" nodes. For example, we can create virtual boats to test most of the system without being physically at a pool.

One more logistical software component present in Fig.1 is the Distributor. The Distributor takes aggregate streams of locations, trajectories, and administrative commands from their respective creators within the central computer and splits them into boat individualized topics. This was done to explicitly control wifi network traffic.

V. ANALYSIS

A. Docking Area

To help ensure that the robots successfully dock when they attempt to use their active docking mechanisms, we have analyzed the set of relative positions where docking is possible. We call this the *area of acceptance*, defined as "the range of possible starting conditions for which mating will be successful" [16]. In this case we consider "mating"
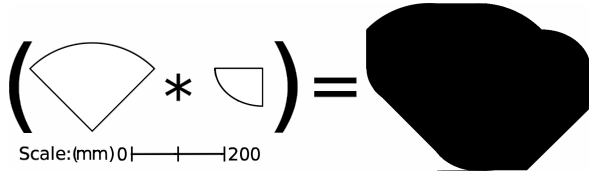
Fig. 6: The docking connector 2D area of acceptance (right) is obtained by convolution of the shape swept out by the hook (left) and the shape swept out by the loop (center).
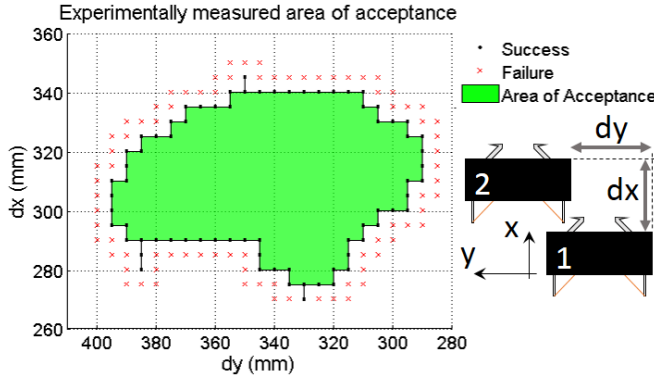

Fig. 7: Experimental data collected to show the actual 2D area of acceptance (boats not drawn to scale).

to be engagement of the hook and loop leading to intimate alignment of two boats in the brick pattern.

Area of acceptance between the two boats is the combination of the areas swept out by the male and female mechanisms. The hook and the loop each sweeps a two dimensional area, shown in Fig. 6. They need only overlap slightly in order to dock. By translating the relative position of the elements in x and y, we can convolve the two area shapes together to create a shape representing the full "area of acceptance". This area was experimentally measured (Fig. 7) and shown to be similar. Relative orientation was also included in our analysis and is handled in a similar manner. One source of error is from the hook tip which is not captured in the convolved image. To help with uncertainty in the positions of two boats while docking, they aim for relative positions corresponding to the center of the area of acceptance. Even with attempts to maximize the area of acceptance, uncertainties from wave and localization errors are enough for docks to sometimes fail (see Section IV-D).

B. Wave and Strength Analysis

In a full scale deployment, one container ship might deploy thousands of modules to form a large conglomerate. We wish the structure to survive in the moderate conditions of sea state three, where a significant wave height of 1.25 m and modal period of 7.5 s might be expected. Requiring a flat chain of 6 m long modules to rigidly "bridge" across such a 88 m swell length anticipates connection moments of 900 kN·m and connection shear forces of up to 300 kN – forces greater than even the considerable weight of the modules themselves. Standard ISO containers are not designed to accept such loading, and in this case compliance to the wave shape is clearly required. Conversely, operational requirements might demand stiffness or shape constraints.

The system addresses these difficulties by incorporating active stiffness connectors between adjoining modules that allows the conglomerate to conform to the wave induced forces reducing structural stress when needed.

While sophisticated wave analysis programs such as Orcaflex can predict hydrodynamic interactions with rigid boats, analyzing the precise effects of buoyancy and waves on the structural properties of a conglomerate made up of a large number of rigid elements connected with compliant docking mechanisms is not tractable as computational complexity explodes. To quickly assess the dynamic response to incoming harmonic waves we developed a method for automatically constructing simple dynamical models for large conglomerates based on an arbitrary connectivity blueprint. These models generate rapid predictions of steady state motions for a proscribed sea state, conglomerate shape, and connection stiffnesses. Such a tool is crucial if an operator wants to take full advantage of the available choices in configuration and stiffness specification while pursuing survivability and operational requirements.

The structural modes of two connected modules free in rotation and translation are governed by their respective 6x6 generalized inertias M along with a 6x6 damping matrix B_c and stiffness matrix C_c, where subscript c indicates these terms are contributed by the connection. The state vectors x_1 and x_2 represent each module as six element vectors giving x, y, z position and roll (about y), pitch (about x), yaw (about z) orientation. For small amplitude rotations the dynamical interaction can be captured by a second order linear ordinary differential equation as in Eqn. (1).

$$\begin{bmatrix} M & 0 \\ 0 & M \end{bmatrix} \begin{bmatrix} \ddot{x_1} \\ \ddot{x_2} \end{bmatrix} + \begin{bmatrix} B_c & -B_c \\ -B_c & B_c \end{bmatrix} \begin{bmatrix} \dot{x_1} \\ \dot{x_2} \end{bmatrix} + \begin{bmatrix} C_c & -C_c \\ -C_c & C_c \end{bmatrix} \begin{bmatrix} x_1 \\ x_2 \end{bmatrix} = 0$$
(1)

A canonical linear formulation for the response of one isolated floating body to small amplitude harmonic waves is similarly described by a second order vectorial Eqn. (2). Matrix coefficients, M, A_w, B_w, and C_w are the 6x6 mass, added mass, added damping, and hydrostatic stiffness matrices where subscript w now denotes that these are contributed by the wave interaction. Finally, $X_w(t)$ is the wave forcing function on the body.

$$(M + A_w)\ddot{x_1} + B_w \dot{x_1} + C_w x_1 = X_w$$
(2)

The added mass matrix A_w gives a linear, six dimensional approximation to the additional inertial effect of the fluid accelerated by the body during small oscillations. Added damping B_w is linear, finite dimensional approximation for the forces resulting from the generation of waves due to the motion of the ship. Matrix C_w captures the hydrostatic contribution to forces on the bodies, which includes the intuitive buoyant force and static righting moments. In general coefficients A_w and B_w are frequency dependent, and we concern ourselves only with the steady state response to harmonic excitation. These terms may be obtained experimentally or, in our case, derived by approximately applying results from strip theory [17].

We assume that neighboring boats interact only through their physical connections and not via hydrodynamic couplings which has shown to be small in multi-module mobile
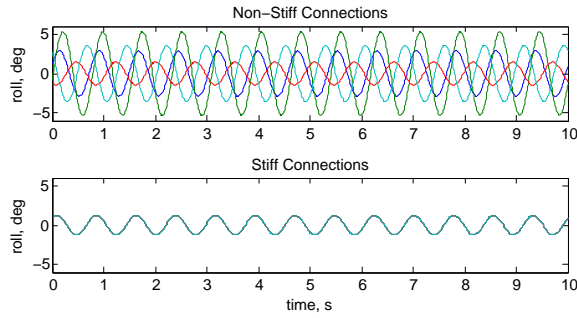
Fig. 8: A simulation of four boats shows that with non-stiff connections the roll angles vary widely, but when stiffened the boats remain aligned and the overall motion is reduced.

offshore bases – though with much larger modules [18]. This permits the wave model of Eqn. 2 to be readily combined with the structural Eqn. 1 by augmenting the inertia, stiffness, and damping terms and introducing the wave forcing. This equation for an interacting pair becomes the building block for programatically assembling the governing equations for large conglomerates as second order differential equations with highly sparse, block structured matrix coefficients.

We applied our model to the 1:12 scale system and compared the numerical results to observations of a four module "diamond" structure in the pool. Waves with an approximate driving period of 0.77 s and amplitude of 2 cm were manually generated, corresponding to wavelengths of 1.8 boat lengths. Simulation of this scenario with stiff connections resulted in negligible relative pitch and roll motions between boats – a result readily confirmed in the pool. Simulations with connections non-stiff in bending display modules moving out of phase with their neighbors, resulting in relative pitch and roll differences between neighbors of up to 8.4^o peak-to-peak (Fig. 8). In the physical experiment, the motions appear qualitatively similar and relative motions in pitch and roll were visually estimated at 6° peak-to-peak. Our simulations additionally predict the conglomerate response may be sensitive to the direction of the incoming wavefront.

C. Docking Geometry

Operational requirements often need the platform to be as smooth as possible, so we wish to minimize vertical shear motions between two modules yet allow other degrees of freedom so that system can comply to wave forces as necessary. To do this, a small rigid shape is added to the hulls surrounding the winch cables. The double cone shape seen in Fig. 9 combines pitch displacement with position displacement. If there is some pitch discrepancy between the boats, the interaction of the mating shapes impose an accompanying positional displacement. Since positional displacement is counteracted by a spring force in the hook-and-loop mechanism, the geometry effectively adds a pitch stiffness term to the 6x6 stiffness matrix.

VI. Experiments

A set of four experiments were run in a large athletic pool (online videos [19]) that verified the following functions:

- multiple aquatic robot trajectory coordination,
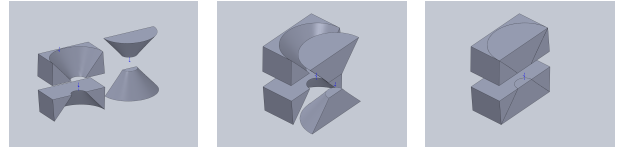- localization across large areas using multiple cameras,

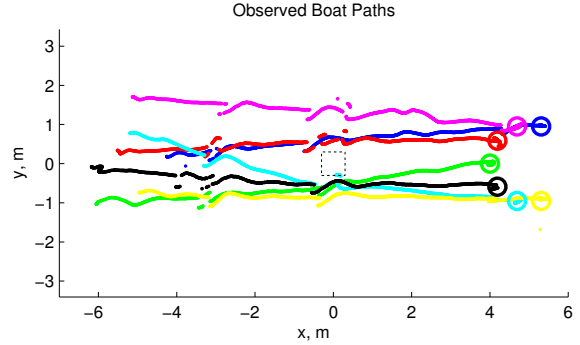Fig. 9: The docking geometry in a pre-docked position, and docked.

Fig. 10: Sensed paths of boats crossing four camera regions. A virtual obstacle (square at 0,0) is avoided.

- docking to free-floating and to land-anchored structures,
- assembly planning for brick-pattern structures, and
- variable structure compliance.

1) Coordinated Undocked Formations: In this experiment a fleet of 10 modules were controlled simultaneously to traverse the pool, avoiding a virtual obstacle and forming a disconnected circular formation on the far side. The fleet crossed through four camera regions. While crossing the seam between two camera regions, misalignments in the seam would cause noticeable control errors. However concurrent control of all three DOF of 10 boats (30 DOF total) was verified.

2) Floating Base: A floating base was automatically formed by six modules. As an additional test, a Pelican quadrotor successfully landed and took off from the island via human control (Fig. 11). Some concerns included the ability of the modules to station-keep in the presence of substantial downwash as well as intermittent loss of localization as the UAV obscured visual markers. These issues did not present a problem.

3) Bridge: To test the assembly planning and scale up the number of modules, 33 modules formed a bridge from
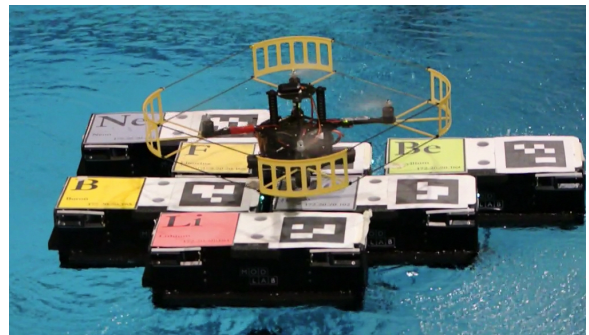

Fig. 11: A quadrotor lands on an island formed of six modules – the same goal shape shown in Fig. 5.
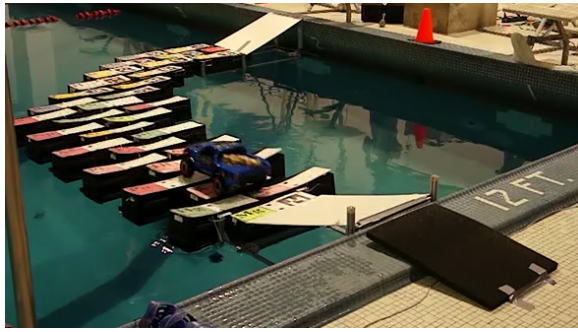
Fig. 12: A bridge of 33 modules spans one corner of the pool. An RC car successfully traverses the bridge.

one side of the pool to another (Fig. 12). Boat modules start the autonomous assembly of the bridge and finish the assembly of the bridge autonomously with partially functioning modules used in-between. The solidity of the bridge was then tested by driving a toy car over the bridge.

One complication comes from the docking of the final element so the bridge spans both sides. The bridge has two land-anchored ends that are ramps to enable boarding and departure from the bridge. Starting the bridge is straight forward building from the end. However, ending the bridge requires docking to two sites simultaneously. In the demonstration, the ramp was placed such that the elements aligned.

The other major issue is the surface characteristics on top of the modules. By having the modules stiff when required, the car had no problem crossing. However, when large gaps formed, wheels would get stuck.

4) Active Stiffness Control: Varying the tightness of the docking mechanism effectively changed the stiffness of a conglomerate of 20 modules. Dynamically changing the stiffness of all 20 modules occurs within one second. The stiffness in roll rotation (modules bending away from one another) due to the padding has been estimated using a linear spring model to be a maximum of 2 kN·m/rad. By loosening the hook and loop mechanism, we can vary the effective stiffness from this value down towards zero as the boats are allowed more freedom to move apart.

VII. Conclusion

This paper presents the key hardware and software challenges in integrating large numbers of identical aquatic vehicles and the first demonstration of modular assembly on water at this scale. The main contributions are the design of the module/boat including the robust docking mechanism, the software architecture that distributed the control and planning computations across all the modules and a central computer, and the algorithms for assembly planning, collision-free trajectory planning, control of multiple moving boats to enable safe navigation and docking. It is worth noting that decomposing the assembly task into three subtasks, (1) docking sequence assembly planning (2) collision-free trajectory planning and (3) physical docking, was important to controlling and coordinating tens of moving boats and demonstrating efficient assembly.

Future work includes improved docking. The demonstrations often required the retries to succeed, making the system less efficient than desired. Maximizing the area of acceptance

for docking is important both for the small scale and full scale system which is designed to handle sea state three. A novel feature of the docking mechanism is the ability to vary the stiffness of the connection between modules. This will enhance the survivability of large structures under harsh wave conditions. A simplified wave and structural strength analysis technique for large numbers of modules is presented to demonstrate this point.

Experiments with multiple full scale containers is a next step in this development. Doing so in a low-cost manner is likely to be an advantage over the earlier MOB approach.

References

[1] (2013, September) DARPA Tactically Expandable Maritime Platform (TEMP). [Online]. Available: http://www.darpa.mil/Our_Work/TTO/Programs/Tactically_Expandable_Maritime_Platform_(TEMP).aspx

[2] F. Mondada, *et al.*, "The cooperation of swarm-bots: Physical interactions in collective robotics," *Robotics & Automation Magazine, IEEE*, vol. 12, no. 2, pp. 21–28, 2005.

[3] Z. Butler, *et al.*, "Generic decentralized control for lattice-based self-reconfigurable robots," *The International Journal of Robotics Research*, vol. 23, no. 9, pp. 919–937, 2004.

[4] W. J. Bender, B. M. Ayyub, and A. Blair, "Assessment of the construction feasibility of the mobile offshore base," in *Int. Workshop on Very Large Floating Structures (VLFS-99), University of Hawaii at Manoa, Honolulu, HI*, vol. 2, 1999, pp. 699–707.

[5] A. R. Girard, J. B. De Sousa, and J. K. Hedrick, "Dynamic positioning concepts and strategies for the mobile offshore base," in *Intelligent Transportation Sys., Proc.* IEEE, 2001, pp. 1095–1101.

[6] J. Seo, M. Yim, and V. Kumar, "Assembly planning for planar structures of a brick wall pattern with rectangular modular robots," in *IEEE Intl. Conf. on Automation Sci. and Eng. (CASE)*, August 2013.

[7] (2013, August) Omap3530-based gumstix overo computer-on-module. [Online]. Available: https://www.gumstix.com

[8] M. Quigley, *et al.*, "ROS: an open-source robot operating system," in *ICRA Workshop on Open Source Software*, 2009.

[9] M. Turpin, N. Michael, and V. Kumar, "Computationally efficient trajectory planning and task assignment for large teams of unlabeled robots," in *Proc. of the IEEE Int. Conf. on Robotics and Automation*, May 2013.

[10] E. Olson, "AprilTag: A robust and flexible visual fiducial system," in *Proceedings of the IEEE International Conference on Robotics and Automation (ICRA)*. IEEE, May 2011, pp. 3400–3407.

[11] C. Feng and V. R. Kamat, "Plane registration leveraged by global constraints for context-aware aec applications," *Computer-Aided Civil and Infrastructure Engineering*, vol. 28, no. 5, pp. 325–343, 2013.

[12] N. Marriott. (2013, April) tmux. [Online]. Available: http://tmux.sourceforge.net

[13] A. Agarwal, M. Slee, and M. Kwiatkowski, "Thrift: Scalable cross-language services implementation," Facebook, Tech. Rep., 4 2007.

[14] K. Varda, "Protocol buffers: Google's data interchange format," Google, Tech. Rep., 6 2008.

[15] M. Quigley, *et al.* (2013, September) ROS comm. [Online]. Available: http://wiki.ros.org/ros_comm

[16] N. Eckenstein and M. Yim, "The x-face: An improved planar passive mechanical connector for modular self-reconfigurable robots," in *Intelligent Robots and Systems (IROS), Proc.*, 2012, pp. 3073–3078.

[17] J. Newman, *Marine Hydrodynamics*. The MIT Press, 1977.

[18] H. Riggs, R. Ertekin, and T. Mills, "Impact of stiffness on the response of a multimodule mobile offshore base," *International Journal of Offshore and Polar Engineering*, vol. 9, no. 2, 1999.

[19] (2013, August) Tactically Expandable Maritime Platform - Highlights. [Online]. Available: http://www.youtube.com/watch?v=2OY3nBtGqVU